Submillimeter Evidence for the Coeval Growth of Massive Black Holes and Galaxy Bulges

M. J. Page,[1]* J. A. Stevens,[1] J. P. D. Mittaz,[1] F. J. Carrera[2]

The correlation, found in nearby galaxies, between black hole mass and stellar bulge mass implies that the formation of these two components must be related. Here we report submillimeter photometry of eight x-ray–absorbed active galactic nuclei that have luminosities and redshifts characteristic of the sources that produce the bulk of the accretion luminosity in the universe. The four sources with the highest redshifts are detected at 850 micrometers, with flux densities between 5.9 and 10.1 millijanskies, and hence are ultraluminous infrared galaxies. If the emission is from dust heated by starbursts, then the majority of stars in spheroids were formed at the same time as their central black holes built up most of their mass by accretion. This would account for the observed demography of massive black holes in the local universe. The skewed rate of submillimeter detection with redshift is consistent with a high redshift epoch of star formation in radio-quiet active galactic nuclei, similar to that seen in radio galaxies.

In the local universe, central black holes are found in most galaxy spheroids (a collective term for elliptical galaxies and the bulges of spiral galaxies) with mass roughly proportional to that of the spheroid (0.13% ± 0.4 dex) (*1*). The simplest explanation for this proportionality is that the black hole mass is built up in active galactic nuclei (AGN) by accretion of the same gas that rapidly forms the stars, which make up the spheroid; i.e., the formation of the spheroid and the growth of the massive black hole are coeval. Assuming that 10% of the spheroid mass M is converted from hydrogen to helium in stars (*2*) at an efficiency of 0.007 and is radiated, and assuming that 0.13% of the spheroid mass M is accreted by the central black hole (*1*) at 10% efficiency, the ratio of radiation emitted by the starburst (E_{SB}) to that emitted by the AGN (E_{AGN}) is

$$\frac{E_{SB}}{E_{AGN}} = \frac{0.1M \times 0.007}{0.0013M \times 0.1} \sim 5 \qquad (1)$$

Hence, if they have similar lifetimes we expect the stellar component to have around 5 times the bolometric luminosity of the AGN during the spheroid formation. A similar argument has been used to estimate the relative contribution of accretion and nuclear fusion to the extragalactic background radiation (*3*). The scatter on this relation for individual objects is expected to be at least 0.4 dex to account for the scatter on the present-day spheroid/black hole mass ratio (*1*), with additional scatter of ~0.3 unit logarithmic interval (dex) from the intrinsic variability of each AGN (*4*).

To investigate this hypothesis, we studied a sample of eight x-ray–absorbed AGN, with redshifts (z) greater than one, that were discovered serendipitously in archival x-ray data (Table 1). They were chosen from the 14 such sources reported (*5*) on the basis of visibility in our allocated observing shifts at the James Clerk Maxwell Telescope (JCMT). If the stellar and black hole components of present-day galaxy spheroids did form at the same time, then the majority of star formation in spheroids must have taken place around the AGN that dominate the universe's accretion power, i.e. those that are responsible for the majority of present-day black hole mass. Our targets are representative of these AGN for four reasons. First, their redshifts span the $1 < z < 3$ epoch in which the accretion luminosity from AGN peaked. For example, in the best-fit luminosity function of a large sample of x-ray selected AGN (*6*), the co-moving AGN x-ray luminosity density is more than a factor of 10 larger at $z = 2$ than in the local universe. Second, their luminosities are close to the break in the luminosity function, which is where the majority of AGN accretion luminosity is produced. For example, in the same model x-ray luminosity function (*6*), 60% of the co-moving AGN x-ray luminosity density is produced by AGN within ±0.5 dex of the break in the luminosity function, which is at $\log L_X = 44.5$ at $z = 2$. Third, the AGN in our sample are x-ray–absorbed. It has been estimated (*7*) that 85% of accretion power in the universe is absorbed, and x-ray background synthesis models require that the majority of AGN be intrinsically absorbed (*8*). Fourth, all but one of them are radio quiet; close to the break in the luminosity function, radio quiet AGN outnumber radio loud AGN by about 15:1 (*9*).

Observations at 850 μm were carried out at the JCMT in excellent, stable weather conditions (*10*) from 18 to 20 January 2001 with the use of the Submillimeter Common User Bolometer Array (SCUBA) (*11*). Four of the eight sources have significant detections (>5 σ) at 850 μm with flux densities between 5.9 and 10.1 mJy; the other four sources were not detected (Table 1). The high submillimeter detection rate for our sources (50%) contrasts with the low rates of detection (≤10%) in previous submillimeter surveys of x-ray selected objects (*12–16*). However, the x-ray sources investigated here have significantly higher x-ray flux (by more than a factor of 3) than the relatively faint x-ray sources in the other surveys. Hence, the faint x-ray sources would probably not be detectable at 850 μm even if they had the same ratio of submillimeter to x-ray flux as our 850 μm detected sources. Although our sample is small, our high detection rate means that at the 99% confidence level, >12% (*16*) of the population from which our sample was drawn are 850 μm sources detectable with SCUBA; at the 95% confidence level, this figure rises to >19%.

We interpret the observed submillimeter flux from all our sources as thermal emission from dust. Because RXJ163308.57+570258.7 is radio loud (*5*), we have also considered (but rejected) the possibility that synchrotron emission contributes to the flux from this source at submillimeter wavelengths. The source has a 1.4-GHz flux density of 17.2 ± 0.7 mJy in the northern Very Large Array sky survey (*17*) and a 325-MHz flux density of 78 ± 4 mJy in the Westerbork northern sky survey (*18*). Therefore, it is a steep spectrum source and, extrapolating the spectrum as a power law, we expect it to contribute an insignificant amount (<0.1 mJy) at 850 μm. We conclude that the observed 850-μm flux of RXJ163308.57+570258.7 is dominated by thermal emission from dust. For all our sources, we estimated the total far infrared (FIR) luminosities L_{FIR} and dust masses M_d (Table 1) from the monochromatic 850-μm fluxes using the FIR spectrum of Mrk 231 as a template. Mrk 231 is appropriate because it is a well-studied, nearby ultraluminous infrared galaxy (ULIRG), which is similar to our AGN in that it hosts an x-ray–absorbed, broad line, active nucleus, and has similar submillimeter luminosity (Fig. 1). We fitted an isothermal, optically thin dust model (*19*) to the FIR data on Mrk 231 (*20*) and obtained a good fit for dust temperature T =

[1]Mullard Space Science Laboratory, University College London, Holmbury St. Mary, Dorking, Surrey RH5 6NT, UK. [2]Instituto de Física de Cantabria (Consejo Superior de Investigaciones Científicas–Universidad de Cantabria), 39005 Santander, Spain.

*To whom correspondence should be addressed. E-mail: mjp@mssl.ucl.ac.uk

44 K, $\beta = 1.55$ (where β is the power law index of the frequency dependence of the dust emissivity) and for FIR luminosity of $3.9 \times 10^{12}\ L_{\odot}$. The FIR luminosities of the four detected AGN qualify them as ULIRGs, and the FIR luminosity of RXJ094144.51+385434.8, in particular, is sufficient for it to be classed as a 'hyperluminous' infrared galaxy (*21*). The current upper limits to the submillimeter fluxes of the four undetected AGN are larger than the flux expected from Mrk 231 at equivalent redshifts (Fig. 1), and therefore it is possible that the entire sample could be ULIRGs.

Recent results from Infrared Space Observatory mid-infrared spectroscopy (*22*), millimeter interferometry (*23*), and detailed radiative transfer modeling (*21*) suggest that massive stars are the dominant power source of around three quarters of nearby ULIRGs (including Mrk 231) and hyperluminous infrared galaxies. For our four sources detected at 850 μm, a comparison of the power output of the AGN to the power emitted in the FIR gives an indication of the relative importance of AGN and starburst heating of the FIR-emitting dust. Assuming that 3% of the bolometric luminosity of an AGN is emitted in the 0.5- to 2-keV band (*24*, *25*), the bolometric luminosities of the AGN in RXJ094144.51+385434.8 and RXJ121803.82+470854.6 are about one-quarter and one-third of their FIR luminosities, respectively, whereas the AGN and FIR luminosities are equivalent (within 0.1 dex) in RXJ124913.86−055906.2 and RXJ163308.57+570258.7. This means that in RXJ094144.51+385434.8 and RXJ121803.82+470854.6, the AGN are not sufficiently powerful to heat the FIR-emitting dust, whereas in the other two cases all of the AGN radiation would have to be absorbed and re-emitted by dust for the AGN to power the FIR emission. Therefore, the low ratios of AGN to FIR luminosity make it very likely that in these sources the FIR is predominantly powered by starlight rather than the central AGN. Our submillimeter detections thus imply that these sources contain massive reservoirs of molecular gas and are producing stars at a prodigious rate ($>1000\ M_{\odot}$ year^{-1}).

The four AGN we detected at 850 μm all have FIR and AGN luminosities similar to what would be expected from Eq. 1 (and this could also be true for the four sources undetected at 850 μm, which is not excluded by the current 850-μm upper limits). Thus, our 850-μm detection rate implies that with 95% confidence, between 19% and 100% of the the population from which our sample is drawn are simultaneously building up their black hole mass by accretion and undergoing intense star formation at rates which are consistent with—indeed suggestive of—the spheroid-AGN formation scenario.

The redshift distribution of our detections is bimodal; all the sources with $z > 1.5$ were detected at 850 μm, whereas none of the sources with $z < 1.5$ were detected at that redshift. This is unlikely to be coincidence. If we split the sample by redshift and assume that the underlying probability of submillimeter detection were independent of redshift, then the probability of detecting all the sources in one redshift bin and detecting none of the sources in the other is <1%. However, the two highest redshift objects in the sample also have the highest x-ray luminosities, and, hence, a correlation between x-ray and submillimeter luminosity could be responsible for the bimodal detection rate. Nonetheless, the skewed detection rate is consistent with the strong dependence of submillimeter luminosity with redshift that has already been found in a sample of radio galaxies (*26*), suggesting that radio galaxies had higher rates of star formation at earlier epochs. Age determinations of stellar bulges in nearby luminous AGN suggest that radio quiet AGN, as well as radio loud AGN, had higher rates of star formation at earlier epochs (*27*). The trend observed in our data is consistent with this hypothesis.

A consequence of coeval spheroid and black hole formation for the recently discovered luminous submillimeter population (*28*) would be that the majority of these sources must host AGN. Indeed, it is already known that a significant fraction of the most luminous submillimeter galaxies found thus far in deep SCUBA surveys contain AGN (*29*). At redshifts of 2 to 3, starbursts with similar bolometric luminosity to AGN with $44 < \log L_X < 45$ would have 850-μm fluxes of ~0.5 to 5 mJy, and this is the flux range in which the bulk of the cosmic 850-μm background is produced (*30*). Current x-ray luminosity functions (*6*, *31*) suggest that there are

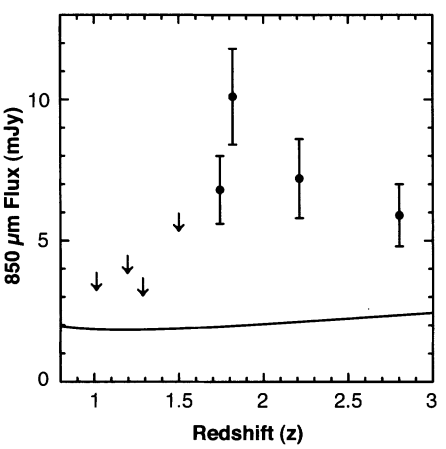

Fig. 1. 850-μm fluxes of the x-ray–absorbed AGN as a function of redshift z. The solid line shows the predicted 850-μm flux of Mrk 231 if it were viewed at redshift z.

Table 1. Characteristics of the observed x-ray–absorbed AGN and their observed submillimeter emission. We assume a Hubble constant $H_0 = 50$ km s^{-1} Mpc^{-1}, a deceleration parameter $q_0 = 0.5$, and zero cosmological constant. For sources that were not detected with SCUBA, we have estimated upper limits to L_{FIR} and M_d by taking the upper limit of S_{850} to be $S_{850} + 2\sigma$ for sources with positive S_{850}, and 2σ for sources with negative S_{850}. Source name is based on *Rosat* position. RXJ124913.86−055906.2 is also known as [HB89] 1246−057, RXJ135529.59+182413.6 is also known as RIXOS F268_011, and RXJ163308.57+570258.7 is also known as WN B1632+5709. S_X, observed 0.5- to 2-keV flux (10^{-14} erg cm^{-2} s^{-1}); log L_X, log [0.5 to 2 keV luminosity (erg s^{-1})] corrected for intrinsic absorption; log N_H, log [intrinsic column density (cm^{-2})]; RL/RQ, radio loud (RL) if the radio-optical spectral index $\alpha_{OR} > 0.35$ or radio quiet (RQ) if $\alpha_{OR} < 0.35$; S_{850}, 850-μm flux. The quoted errors do not include calibration uncertainties of 10%. Dust mass inferred from 850-μm flux adopts a value for the dust mass absorption coefficient (*33*) $\kappa_{100\mu m} = 5.5$ m^2 kg^{-1}. L_{FIR}, FIR luminosity inferred from 850-μm flux.

Source	z	S_x	log L_x	log N_H	RL/RQ	$S_{850\ (mJy)}$	Dust mass ($M_{\odot}$)	$L_{FIR}(L_{\odot})$
RXJ094144.51+385434.8	1.819	$2.1^{+0.5}_{-0.5}$	44.8 ± 0.1	$21.9^{+0.5}_{-0.4}$	RQ	10.1 ± 1.7	1.2×10^9	2.0×10^{13}
RXJ101123.17+524912.4	1.012	$3.3^{+1.0}_{-0.9}$	44.7 ± 0.2	$22.5^{+0.2}_{-0.3}$	RQ	−1.4 ± 1.9	$< 4.7 \times 10^8$	$< 8.0 \times 10^{12}$
RXJ104723.37+540412.6	1.500	$1.7^{+0.7}_{-0.6}$	44.6 ± 0.2	$22.2^{+0.4}_{-0.6}$	RQ	2.3 ± 1.8	$< 7.2 \times 10^8$	$< 1.2 \times 10^{13}$
RXJ111942.16+211518.1	1.288	$3.4^{+0.6}_{-0.5}$	44.6 ± 0.1	$21.4^{+0.4}_{-0.3}$	RQ	−0.9 ± 1.8	$< 4.5 \times 10^8$	$< 7.6 \times 10^{12}$
RXJ121803.82+470854.6	1.743	$1.5^{+0.4}_{-0.4}$	44.7 ± 0.2	$22.3^{+0.3}_{-0.7}$	RQ	6.8 ± 1.2	8.0×10^8	1.4×10^{13}
RXJ124913.86−055906.2	2.212	$2.4^{+0.5}_{-0.4}$	45.1 ± 0.1	$22.2^{+0.4}_{-0.6}$	RQ	7.2 ± 1.4	7.8×10^8	1.3×10^{13}
RXJ135529.59+182413.6	1.196	$3.6^{+0.9}_{-0.9}$	44.7 ± 0.2	$22.2^{+0.2}_{-0.5}$	RQ	0.8 ± 1.3	$< 4.3 \times 10^8$	$< 7.2 \times 10^{12}$
RXJ163308.57+570258.7	2.802	$1.9^{+0.3}_{-0.3}$	45.2 ± 0.1	$22.5^{+0.3}_{-0.5}$	RL	5.9 ± 1.1	5.8×10^8	9.8×10^{12}

at least several hundreds of AGN deg^{-2} with $z > 1$ and $\log L_X > 44$, assuming a 4:1 ratio of obscured to unobscured sources. Although this estimation falls well short of the current 850-μm source counts (8000 ± 3000 deg^{-2} at 1 mJy) (*30*), the AGN x-ray luminosity function has a large uncertainty at $z > 2$, which is the epoch in which the majority of luminous submillimeter galaxies are found (*32*). Furthermore, the space density of obscured AGN at high redshift is unknown: the x-ray background intensity does not preclude the existence of a large population of high redshift, Compton-thick sources.

References and Notes

1. J. Kormendy, K. Gebhardt, in *The 20th Texas Symposium on Relativistic Astrophysics*, H. Martel, J. C. Wheeler, Eds. (American Institute of Physics, in press) (e-Print available at http://xxx.lanl.gov/abs/astro-ph/0105230).
2. M. Schönberg, S. Chandrasekhar, *Astrophys. J.* **96**, 161 (1942).
3. G. Hasinger, in *ISO Surveys of a Dusty Universe*, D. Lemke, M. Stickel, K. Wilke, Eds. (Springer, New York, in press) (e-Print available at http://xxx.lanl.gov/abs/astro-ph/0001360).
4. M. R. S. Hawkins, *Astron. Astrophys. Suppl.* **143**, 465 (2000).
5. M. J. Page, J. P. D. Mittaz, F. J. Carrera, *Mon. Not. R. Astron. Soc.* **325**, 575 (2001).
6. M. J. Page, K. O. Mason, I. M. McHardy, L. R. Jones, F. J. Carrera, *Mon. Not. R. Astron. Soc.* **291**, 324 (1997).
7. A. C. Fabian, K. Iwasawa, *Mon. Not. R. Astron. Soc.* **303**, L34 (1999).
8. R. Gilli, G. Risaliti, M. Salvati, *Astron. Astrophys.* **347**, 424 (1999).
9. P. Ciliegi *et al.*, *Mon. Not. R. Astron. Soc.* **277**, 1463 (1995).
10. Observations were carried out in photometry mode using a standard chop/nod/jiggle observing technique. The atmospheric transmission and "submillimeter seeing" were at all times in the top quartile of values measured on Mauna Kea ($\tau < 0.2$, seeing < 0.5 arcsec). STARLINK SURF software was used to correct for the nod, flatfield, extinction, and despike and to remove sky noise from the data. Flux calibration was made against the primary submillimeter calibrator, Mars.
11. W. S. Holland *et al.*, *Mon. Not. R. Astron. Soc.* **303**, 659 (1999).
12. A. E. Hornschemeier *et al.*, *Astrophys. J.* **554**, 742 (2001).
13. A. J. Barger, L. L. Cowie, R. F. Mushotzky, E. A. Richards, *Astron. J.*, **121**, 662 (2001) (e-Print available at http://xxx.lanl.gov/abs/astro-ph/0007175).
14. P. Severgnini *et al.*, *Astron. Astrophys.* **360**, 457 (2000).
15. A. C. Fabian *et al.*, *Mon. Not. R. Astron. Soc.* **315**, L8 (2000).
16. N. Gehrels, *Astrophys. J.* **303**, 336 (1986).
17. J. J. Condon *et al.*, *Astron. J.* **115**, 1693 (1998).
18. R. B. Rengelink *et al.*, *Astron. Astrophys. Suppl.* **124**, 259 (1997).
19. R. D. Hildebrand, *Q. J. R. Astron. Soc.* **24**, 267 (1983).
20. D. Rigopoulou, A. Lawrence, M. Rowan-Robinson, *Mon. Not. R. Astron. Soc.* **278**, 1049 (1996).
21. M. Rowan-Robinson, *Mon. Not. R. Astron. Soc.* **316**, 885 (2000).
22. R. Genzel *et al.*, *Astrophys. J.* **498**, 579 (1998).
23. D. Downes, P. M. Solomon, *Astrophys. J.* **507**, 615 (1998).
24. M. Elvis *et al.*, *Astrophys. J. Suppl.* **95**, 1 (1994).
25. If our objects are systematically underluminous in x-rays, then we would be underestimating the bolometric luminosities of their active nuclei. However, this is unlikely because these sources were found in an x-ray survey, in which the natural selection bias is expected to favor sources with higher-than-average x-ray to bolometric luminosity ratios rather than lower-than-average ones.
26. E. N. Archibald *et al.*, *Mon. Not. R. Astron. Soc.* **323**, 417 (2001).
27. L. A. Nolan *et al.*, *Mon. Not. R. Astron. Soc.* **323**, 308 (2001).
28. I. Smail, R. J. Ivison, A. W. Blain, *Astrophys. J.* **490**, L5 (1997).
29. R. J. Ivison *et al.*, *Mon. Not. R. Astron. Soc.* **315**, 209 (2000).
30. A. W. Blain, J.-P. Kneib, R. J. Ivison, I. Smail, *Astrophys. J.* **512**, L87 (1999).
31. T. Miyaji, G. Hasinger, M. Schmidt, *Astron. and Astrophys.* **369**, 49 (2001).
32. J. S. Dunlop, *N. Astron. Rev.* **45**, 609 (2001).
33. B. T. Draine, H. M. Lee, *Astrophys. J.* **285**, 89, (1984).

34. The JCMT is operated on behalf of the Particle Physics and Astronomy Research Council of the United Kingdom, the Netherlands Organization for Scientific Research, and the National Research Council of Canada.

31 August 2001; accepted 16 October 2001
Published online 1 November 2001;
10.1126/science.1065880
Include this information when citing this paper.

Fermi Surface Sheet–Dependent Superconductivity in 2*H*-$NbSe_2$

T. Yokoya,[1]* T. Kiss,[1] A. Chainani,[1,2] S. Shin,[1,3] M. Nohara,[4] H. Takagi[4]

High-resolution angle-resolved photoemission spectroscopy was used to study the superconducting energy gap and changes in the spectral function across the superconducting transition in the quasi–two-dimensional superconductor 2*H*-$NbSe_2$. The momentum dependence of the superconducting gap was determined on different Fermi surface sheets. The results indicate Fermi surface sheet–dependent superconductivity in this low–transition temperature multiband system and provide a description consistent with thermodynamic measurements and the anomalous de Haas–van Alphen oscillations observed in the superconducting phase. The present data suggest the importance of Fermi surface sheet–dependent superconductivity in explaining exotic superconductivity in other multiband systems with complex Fermi surface topology, such as the borides and f-electron superconductors.

The energy gap in the single-particle excitation spectrum of the superconducting state makes the superconducting properties of a material qualitatively different from its normal-state properties. BCS (Bardeen, Cooper, and Schrieffer) theory (*1*) assumes electron-electron pairing to be due to phonons and approximates the pairing strength as a function of momentum to be constant, leading to an isotropic s-wave gap. This is not the case for high–transition temperature superconductors (high-T_c's), where a highly anisotropic $d_{x^2-y^2}$ gap has been confirmed (*2*, *3*) and unconventional pairing mechanisms other than electron-phonon interaction are actively considered (*4*). On the other hand, even for phonon-mediated s-wave superconductors, the existence of several Fermi surface (FS) sheets possessing different electron-phonon coupling constants and/or differing density of states (DOS) at the Fermi level (E_F) can give rise to a momentum-dependent superconducting gap in real materials (*5*, *6*). However, although tunneling studies (*5*) have deduced a momentum-dependent gap from momentum-averaged spectra, there is no direct experimental evidence based on momentum-resolved spectra to substantiate that claim.

We show that the electronic structure of 2*H*-$NbSe_2$ (*7*), a quasi–two-dimensional incommensurate charge density wave (CDW) system ($T_{CDW} \sim 35$ K) that is also a phonon-mediated superconductor below $T_c = 7.2$ K, exhibits FS sheet–dependent superconductivity. The result highlights the importance of FS sheet dependence of electronic structure and electron-phonon interactions in low-T_c superconductors.

Angle-resolved photoemission spectroscopy (ARPES) allows determination of the energy and momentum distribution of occupied electrons in a solid. For a given energy of incident photons, the energy distribution curve (EDC) measured at a fixed momentum and, conversely, the momentum distribution curve (MDC) measured at a fixed energy, directly represent the nature of the electronic states of a system. Thus, typically, ARPES can measure the Fermi momentum (k_F) as the point in momentum space corresponding to a band crossing E_F, with the locus of measured k_F's forming a Fermi surface. At a selected momentum vector on a FS, a temperature-dependent ARPES study can also measure the opening of a superconducting gap in the

[1]Institute for Solid State Physics, University of Tokyo, Kashiwa, Chiba 277-8581, Japan. [2]Institute for Plasma Research, Bhat, Gandhinagar-382 428, India. [3]The Institute of Physical and Chemical Research (RIKEN), Sayo-gun, Hyogo 679-5143, Japan. [4]Department of Advanced Materials Science, University of Tokyo, Tokyo 113-0033, Japan.

*To whom correspondence should be addressed. E-mail: yokoya@issp.u-tokyo.ac.jp